Featured in Physics

First Study of the ^{139}Ba$(n,\gamma)^{140}$Ba Reaction to Constrain the Conditions for the Astrophysical *i* Process

A. Spyrou,[1,2,3,*] D. Mücher,[4,5,6,†] P. A. Denissenkov,[7,‡] F. Herwig,[7,‡] E. C. Good,[1,3] G. Balk,[8] H. C. Berg,[1,2,3] D. L. Bleuel,[9] J. A. Clark,[10] C. Dembski,[1,2,3] P. A. DeYoung,[8] B. Greaves,[5] M. Guttormsen,[11] C. Harris,[1,2,3] A. C. Larsen,[11] S. N. Liddick,[1,12] S. Lyons,[13] M. Markova,[11] M. J. Mogannam,[1,12] S. Nikas,[14] J. Owens-Fryar,[1,2,3] A. Palmisano-Kyle,[15] G. Perdikakis,[16] F. Pogliano,[11] M. Quintieri,[1,2] A. L. Richard,[9] D. Santiago-Gonzalez,[10] G. Savard,[10] M. K. Smith,[1,3] A. Sweet,[9] A. Tsantiri,[1,2,3] and M. Wiedeking[17,18]

[1]*Facility for Rare Isotope Beams, Michigan State University, East Lansing, Michigan 48824, USA*
[2]*Department of Physics and Astronomy, Michigan State University, East Lansing, Michigan 48824, USA*
[3]*Joint Institute for Nuclear Astrophysics, Michigan State University, East Lansing, Michigan 48824, USA*
[4]*Institute for Nuclear Physics, University of Cologne, 50937 Köln, Germany*
[5]*Department of Physics, University of Guelph, Guelph, Ontario N1G 2W1, Canada*
[6]*TRIUMF, 4004 Wesbrook Mall, Vancouver, British Columbia, Canada V6T 2A3*
[7]*Department of Physics & Astronomy, University of Victoria, Post Office Box 1700, STN CSC, Victoria, British Columbia V8W2Y2, Canada*
[8]*Department of Physics, Hope College, Holland, Michigan 49422-9000, USA*
[9]*Lawrence Livermore National Laboratory, 7000 East Avenue, Livermore, California 94550-9234, USA*
[10]*Physics Division, Argonne National Laboratory, Argonne, Illinois 60439, USA*
[11]*Department of Physics, University of Oslo, NO-0316 Oslo, Norway*
[12]*Department of Chemistry, Michigan State University, East Lansing, Michigan 48824, USA*
[13]*Pacific Northwest National Laboratory, Richland, Washington 99352, USA*
[14]*University of Jyväskyla, Accelerator Laboratory, Department of Physics 11 Post Office Box 35, FI-40014 University of Jyväskyla, Finland*
[15]*Department of Physics and Astronomy, University of Tennessee, Knoxville, Tennessee 37996, USA*
[16]*Department of Physics, Central Michigan University, Mount Pleasant, Michigan 48859, USA*
[17]*SSC Laboratory, iThemba LABS, Post Office Box 722, Somerset West 7129, South Africa*
[18]*School of Physics, University of the Witwatersrand, Johannesburg 2050, South Africa*

(Received 31 January 2023; revised 6 June 2023; accepted 4 April 2024; published 17 May 2024)

New astronomical observations point to a nucleosynthesis picture that goes beyond what was accepted until recently. The intermediate "*i*" process was proposed as a plausible scenario to explain some of the unusual abundance patterns observed in metal-poor stars. The most important nuclear physics properties entering *i*-process calculations are the neutron-capture cross sections and they are almost exclusively not known experimentally. Here we provide the first experimental constraints on the ^{139}Ba$(n,\gamma)^{140}$Ba reaction rate, which is the dominant source of uncertainty for the production of lanthanum, a key indicator of *i*-process conditions. This is an important step towards identifying the exact astrophysical site of stars carrying the *i*-process signature.

DOI: 10.1103/PhysRevLett.132.202701

The synthesis of elements heavier than iron has been an open scientific question for over six decades [1,2]. It is a complex problem that requires input from many different fields, from astronomy, astrophysics, and nuclear physics, to atomic physics, and beyond. The classical picture involves three main processes to produce all isotopes of the heavy elements: the slow (*s*) [3] and rapid (*r*) processes [4–6], through sequences of neutron-capture reactions and β decays, and the p process mainly through photodisintegration reactions [1,7].

While this picture was considered rather complete for a long time, recent astronomical observations point to the need for additional sources to produce heavy elements. In 1977, Cowan and Rose [8] proposed an intermediate (*i*) process that could be triggered in stars with neutron densities $N_n = 10^{13}$–10^{15} n/cm^3, intermediate between those typical for the *s* process ($N_n \lesssim 10^{12}$ n/cm^3) and *r* process ($N_n \gtrsim 10^{20}$ n/cm^3). Recently, astronomical observations of carbon-enhanced metal-poor (CEMP) stars revealed that some of them appeared to have abundance patterns that could not be explained by the classic picture [9–16].

From an astrophysics perspective, an *i* process could take place in conditions where both hydrogen- and

helium-induced reactions can occur together in a single convection zone. This way the neutron-producing reaction $^{13}C(\alpha,n)^{16}O$ is accompanied by the enrichment of ^{13}C via the $^{12}C(p,\gamma)^{13}N(e^{+}\nu)^{13}C$ sequence, resulting in higher neutron densities. This can be possible during a He flash when convection driven by helium burning mixes primary ^{12}C with hydrogen from the surrounding hydrogen-rich envelope. Such conditions are possible in thermally pulsing asymptotic giant branch (AGB) and post-AGB stars, as well as in rapidly accreting white dwarfs (RAWDs) [8,17–24], super-AGB stars [13], the core-He flash in low-mass stars [25], or possibly in massive stars [26]. It should be noted that elements all the way up to the barium region can only be reached if these intermediate neutron-densities are sustained long enough to reach high neutron exposures [24,27]. A recent study showed that under *i*-process conditions in AGB stars, the flow could extend even into the actinide region, producing Th and U [28].

To investigate which neutron density within the *i*-process regime was responsible for the heavy element production as observed in a given set of CEMP stars, we followed the prescription of Denissenkov *et al.* [22,27,29]. Under *i*-process conditions, the flow involves nuclei that are 3 to 7 neutrons away from the last stable isotope of each element. For these nuclei the production uncertainties are dominated by the unknown neutron capture rates of a small number of reactions [22,27,29]. In the approach used here (as in Refs. [22,27,29]) the nuclear reaction rates were varied independently for each reaction, and their impact on the final abundances was investigated. Other studies, e.g., Ref. [30], highlight the fact that theoretical model predictions exhibit strong correlations in reaction rates for neighboring nuclei. While this is indeed the case in the theoretical models, experimental results do not always follow those trends, e.g., Ref. [31], justifying the variation of individual reaction rates independently.

In the present work we investigate the production of lanthanum (La). La is one of the elements for which a large number of stellar observation data is available. La/Eu has been used traditionally to distinguish between the *s* and *r* processes, while enhanced Ba/La has been observed in metal-poor stars beyond *s* and *r* process values, making it a possible *i*-process identifier. At the considered neutron density the uncertainties are dominated by the reaction $^{139}Ba(n,\gamma)^{140}Ba$ [27,32]. ^{139}Ba has a half-life of 83 min, which makes it extremely challenging to measure this reaction directly in the laboratory. We present the first experimental constraint for this reaction using indirect techniques [33–36] and investigate the impact on the production of La within the *i* process.

The $^{139}Ba(n,\gamma)^{140}Ba$ reaction rate was previously predicted purely based on theoretical calculations within the Hauser-Feshbach statistical model [37]. Within this model the nucleus is described using statistical properties, namely, the nuclear level density (NLD), i.e., the number of levels per unit energy for each excitation energy, and the γ-ray strength function (γSF), which represents the reduced probability of γ-ray emission of certain multipolarity and energy. The variation in the calculated $^{139}Ba(n,\gamma)^{140}Ba$ reaction rate was estimated in [27] using the open source code TALYS1.6 [38] to be a factor of ≈6. In our recent work [36] we showed that this is probably an underestimation of the theoretical uncertainty, which could reach an order of magnitude, or more. Here we provide the first experimental constraints on the NLD and γSF of ^{140}Ba, and in this way significantly reduce the uncertainties associated with the $^{139}Ba(n,\gamma)^{140}Ba$ reaction. It should be noted that for *i*-process temperatures no significant thermal excitations are expected [39–41], hence only the neutron capture on the ground state of ^{139}Ba was taken into account here.

The experiment took place at Argonne National Laboratory using a ^{140}Cs beam produced by the CARIBU facility. The ^{140}Cs beam was delivered to the center of the Summing NaI (SuN) detector [42], which is a γ-ray total absorption spectrometer developed at Michigan State University. The beam was implanted in the SuNTAN tape transport system, although the tape was not moved due to the large difference in half-life between the parent isotope ^{140}Cs ($T_{1/2} = 63.7$ s) and the child ^{140}Ba ($T_{1/2} = 12.7d$). Gamma rays in SuN were measured in coincidence with β particles detected by a plastic scintillator barrel detector surrounding the implantation point. The light emitted by the plastic scintillator was collected by 32 wavelength-shifting fiber optics, embedded in the plastic, and transported to two photomultiplier tubes outside of SuN.

SuN is divided into eight optically isolated segments. The energy deposited in each of the segments is sensitive to the individual γ rays (E_γ) emitted from the dexcitation of the child nucleus ^{140}Ba. At the same time, summing up the energy deposited in the whole detector gives information on the excitation energy of the child nucleus (E_x). Combining the E_x and E_γ in a two-dimensional matrix, is the starting point of this analysis [33], as shown in Fig. 1, top.

The details of the experimental techniques and analysis were presented in [36] and include the β-Oslo method [33,34] and shape method [35,36]. In short, the Oslo method involves the unfolding of the $E_x - E_\gamma$ matrix (Fig. 1, top) with the detector response [43], and then applying an iterative subtraction process to extract the first-generation γ-ray distribution [43]. This first-generation matrix was then used to extract the functional form of the NLD and γSF [33,34,44,45]. In addition, the shape method [35,36] was applied to the feeding of the first two 2^+ states of ^{140}Ba at energies 602 and 1511 keV to extract the γ-ray energy dependence or shape of the γSF. The resulting γSF is shown in Fig. 1, (bottom, blue squares). In the same figure the γSF in the giant dipole resonance (GDR) region is shown for the neighboring isotope ^{138}Ba (taken from [46–48]). In addition, the eight default γSF

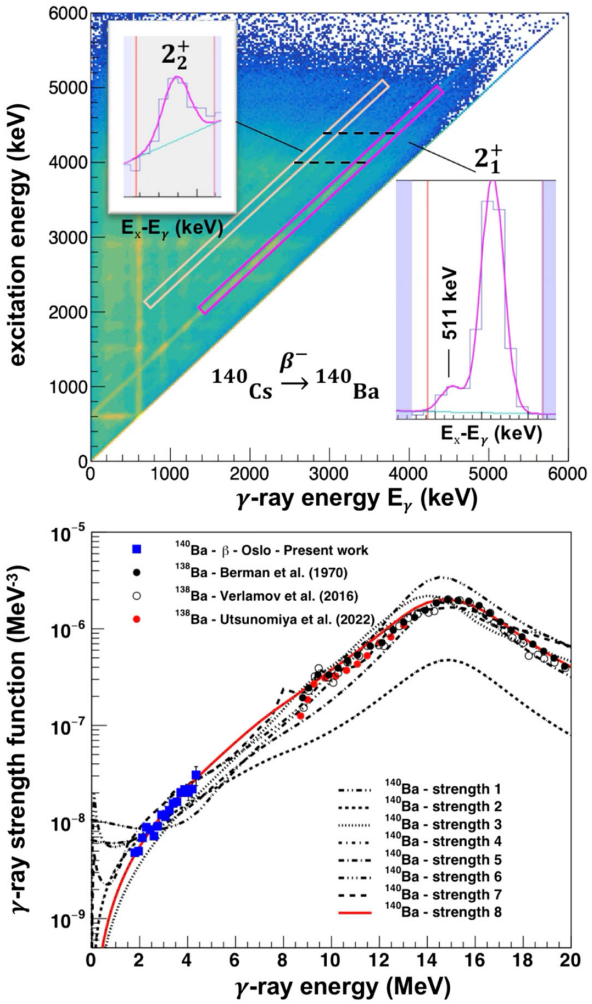

FIG. 1. Top: Raw matrix of γ-ray energies and excitation energies following β decay of ^{140}Cs. The two diagonal projections for excitation energies 4.0–4.4 MeV are shown as insets together with their fits. Bottom: γSF extracted in the present work (blue squares) compared to data for ^{138}Ba at higher energies (black, white, and red dots), as well as theoretical models taken from TALYS1.95.

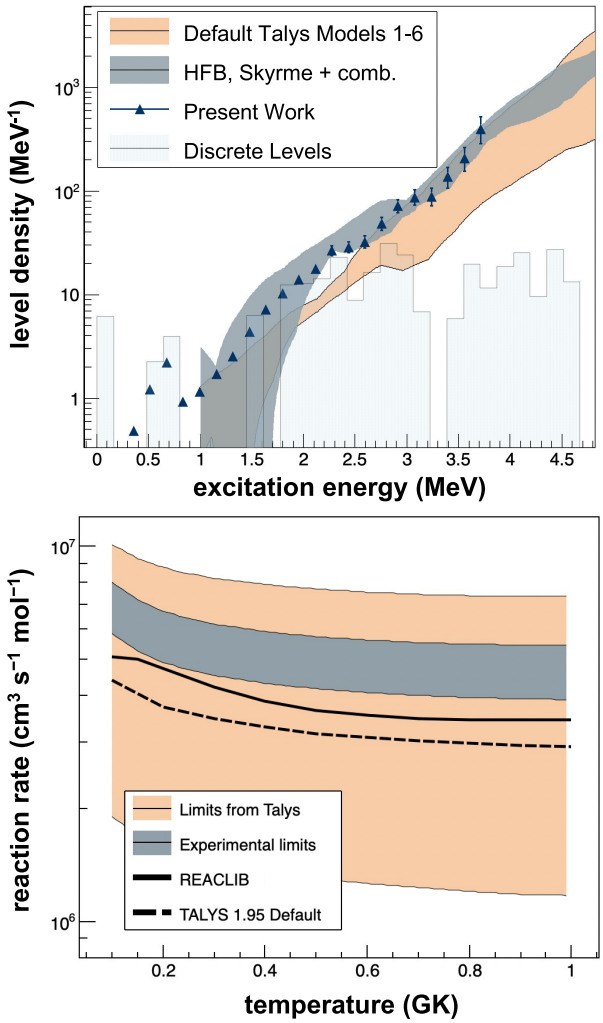

FIG. 2. Top: NLD extracted in the present work (triangles) together with the known discrete levels (light-blue shaded histogram) and theoretical calculations available in TALYS1.95 (orange band). The gray band corresponds to a fit of the present data using ldmodel 5 [55]. Bottom: Reaction rate of the ^{139}Ba$(n,\gamma)^{140}$Ba reaction. The gray band represents the experimentally constrained reaction rate extracted in the present work. The orange band shows the range of predicted reaction rates from the TALYS1.6 calculations that were considered the uncertainty for this reaction in [27]. The solid black line corresponds to the default value used in [27] taken from the JINA-REACLIB [56], and the black-dashed line to the TALYS1.95 calculation with default parameters. It should be noted that a calculation with the same default parameters using TALYS1.6 results in the same reaction rate within 1.5%.

models available in TALYS1.95 are also shown for comparison. Our analysis cannot constrain the absolute magnitude of the extracted γSF, therefore our results were scaled to match the amplitude of each model to allow for a comparison of the γ-ray energy dependence of the different models. Several models could be rejected due to the different energy dependence (models 1,2,4,5,6). The best match to all experimental data is TALYS1.95 strength 8, which corresponds to a Hartree-Fock-Bogolyubov plus quasiparticle random phase approximation (QRPA) based on the Gogny D1M interaction [49]. This was also the proposed model in [48]. Based on these results, TALYS1.95 strength 8 was used for the determination of the neutron-capture reaction cross section. Models 3 and 7 in Fig. 1 could not be excluded. The change in the extracted reaction cross section compared to using model 8 was only 30%–40%. Finally, it should be noted that the experimental data do not exhibit the presence of a low energy enhancement (LEE), as observed in some other nuclei [50], with major impact on neutron-capture cross sections [51]. Recently the LEE was shown to weaken when moving away from closed shells [52], therefore the lack of a LEE in ^{140}Ba, only two neutrons away from the $N = 82$ closed shell, is surprising. Additional investigations are needed to

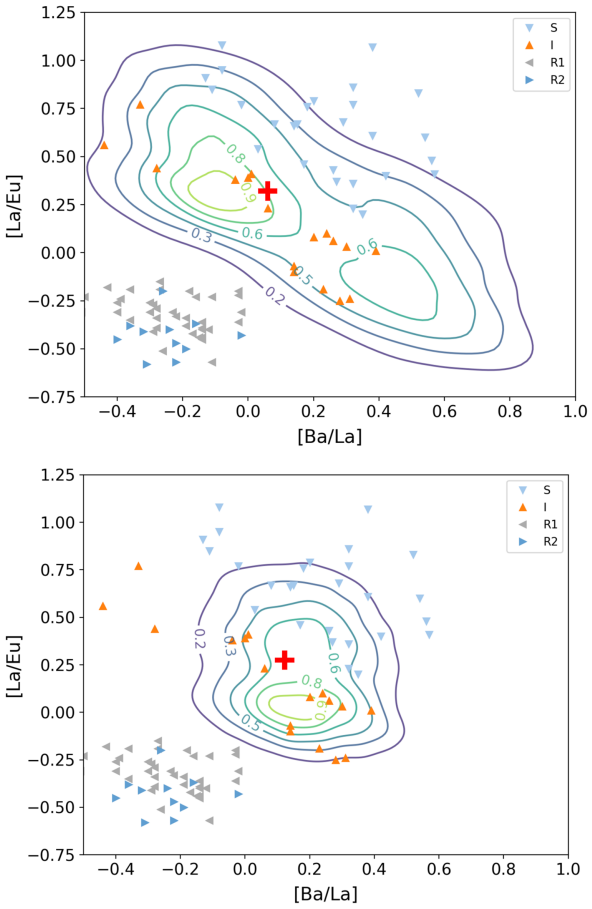

FIG. 3. Top panel: The observed [La/Eu] versus [Ba/La] abundance ratios in CEMP stars taken from the JINABase [58]. Capital letters used in legends indicate how the stars are classified in JINAbase according to the criteria of Table 2 in [59]. *S* indicates CEMP-*s* stars (CEMP stars enhanced in *s*-process elements), *I* stands for CEMP-*s*/*r* stars, while R1 and R2 for two categories of CEMP-*r* stars. The contours show the probability distribution of these abundance ratios predicted in our MC simulations for the constant neutron density $N_n = 3.16 \times 10^{13}$ n/cm^3 as described in [27]. Bottom panel: Same as top panel, but with the ^{139}Ba$(n,\gamma)^{140}$Ba reaction rate and its significantly reduced uncertainty taken from the present work. In both panels, the red crosses display abundance ratios for the corresponding calculations that used the default rates for all reactions from the JINA-REACLIB [56]. Error bars were omitted from the observations to improve the clarity of the figure. Note: the bracket notation $[X/Y]$ represents the logarithmic ratio of the element ratio in the star divided by the element ratio in the sun.

understand this phenomenon and its impact on astrophysical processes.

Once the γ-ray energy dependence of the γSF was fixed from the shape method, it was further used to also fix the slope of the NLD in the β-Oslo method [36] (Fig. 2, top, blue triangles). The absolute amplitude of the NLD was determined using the known discrete levels (light blue shaded area). While RIPL3 [53] considers the level scheme to be complete up to excitation energy 2.87 MeV, our results show that this energy is most probably too high. This also explains the discrepancy with the default NLD models (orange band in Fig. 2) since some of them are normalized to discrete levels up to the RIPL3 recommend value. A similar behavior was observed in the case of ^{88}Kr and discussed in more detail in Ref. [36]. It should be noted that the NLD extracted with this technique is only partial and corresponds to spins $J = 0$–3 of both parities. This range was calculated by assuming allowed β-decay transitions from the 1^- ground state of ^{140}Cs followed by dipole γ-ray emission. Converting the partial NLD to a full NLD requires theory input. However, the fact that all NLD models in TALYS1.95 predict the particular spin range to be of the order of 23%–27% of the full NLD at the neutron separation energy suggests that the uncertainty due to the spin distribution is smaller than other sources of uncertainty. The impact of the partial spin population in β decay was investigated in Ref. [54].

Figure 2, top, also shows the range of theoretical predictions using the six NLD models available in TALYS1.95 (orange band). Here we fit the RIPL3 recommended NLD model (ldmodel 5 in TALYS1.95 from [55]) to our experimental results following the method described in Ref. [36], and the extracted uncertainty band is shown in the gray color.

Using our data we extracted an experimentally-constrained neutron-capture cross section, as shown in Fig. 2, (bottom, gray shaded area), using TALYS1.95 with default parameters, except for the NLD and γSF. For comparison, the theoretical predictions using all available NLD and γSF models in TALYS1.6 are shown as an orange band (taken from [27]). It can be seen that the range of the predicted cross section is greatly reduced. In addition, we compare to the default reaction rate from the JINA REACLIB V1.1 [56] (solid black line), which is commonly used in astrophysical calculations, including [27]. It can be observed that the experimental reaction rate is overall higher than the default value.

The new experimentally constrained reaction rate was used in astrophysical *i*-process calculations to investigate its impact on the final abundance patterns. The calculations were done using a network code that was configured to impose a constant neutron density as was done previously in [27]. While a one-zone model is rather simplistic, it is expected to be realistic when compared to stars with strongly enhanced *i*-process elements. Indeed, complex multizone advective-two-stream postprocessing of 3D hydrodynamic simulations of the *i* process in RAWDs [57] confirms this assumption. Therefore ratios of nearby heavy elements, such as in the region from Ba to Eu, are almost equally well reproduced with equilibrium network solutions if the same neutron density is imposed as the maximum neutron density obtained in the astrophysical simulation. Equilibrium models are preferred because they provide a site-independent elemental ratio estimate

depending only on the neutron density. This way the investigation can focus on the impact of nuclear physics for any site where the given neutron density dominates.

We studied the impact of reaction rate uncertainties on predicted abundances using Monte Carlo (MC) simulations in which rates of selected reactions are varied within their uncertainty ranges. Then, correlations are sought between roughly 10000 abundances predicted in these MC runs for a given element and reaction rate variation factors. This method was used by [27] to reveal a strong negative correlation between the La abundance and the rate of the reaction $^{139}\mathrm{Ba}(n,\gamma)^{140}\mathrm{Ba}$ at $\mathrm{N}_n = 3.16 \times 10^{13}$ n/cm^3 corresponding to conditions found in RAWD models [23]. Here we have performed MC calculations using the default JINA REACLIB rates [56] and their uncertainties for an extended set of 431 (n,γ) reactions relevant for the *i*-process nucleosynthesis and extracted the probability distribution of the predicted abundance ratios [La/Eu] and [Ba/La] that is shown in the top panel of Fig. 3. In the same panel the results are compared to observations of stars from the JINABase [58]. It can be observed that while the neutron density of 3.16×10^{13} n/cm^3 could reproduce these abundance ratios, the large uncertainties associated with the calculations hinder our ability to identify which specific stars (if any) are produced at this particular density.

The rate of the $^{139}\mathrm{Ba}(n,\gamma)^{140}\mathrm{Ba}$ reaction extracted in the present work is overall higher than the default JINA REACLIB value. More importantly the resulting uncertainty is significantly reduced. As a result, the corresponding probability distribution in the abundance plot is substantially tighter, as shown in the bottom panel in Fig. 3. This is a significant result as we can now identify groups of stars that are candidates associated with the neutron density typical in RAWD models.

With the $^{139}\mathrm{Ba}(n,\gamma)^{140}\mathrm{Ba}$ uncertainty reduced, one can investigate the source of the remaining asymmetry in the probability distribution of Fig. 3, bottom panel. We find that the reaction $^{151}\mathrm{Nd}(n,\gamma)^{152}\mathrm{Nd}$ has a strong negative correlation with the predicted abundance of Eu, as already mentioned in the sensitivity study of Denissenkov *et al.* [27].

In summary, the present work reports on the first experimental constraint of the $^{139}\mathrm{Ba}(n,\gamma)^{140}\mathrm{Ba}$ reaction rate using the β-Oslo and shape methods. The resulting rate is used in astrophysical *i*-process calculations which show that the uncertainty in the predictions for the double abundance ratio of [La/Eu] and [Ba/La] is greatly reduced, and is now comparable to the uncertainties from astronomical observations. With this result we have been able to narrow down the group of stars out of the JINAbase that most likely have experienced neutron densities associated with RAWD simulations, which will be a stepping stone for further investigations of this astrophysical site. Finally, we showed that the measurement of a single neutron-capture reaction rate can have a large impact in the predictions of *i*-process models, and we therefore encourage more such measurements in the future.

This research used resources of ANL's ATLAS facility, which is a DOE Office of Science User Facility. The work was supported by the National Science Foundation under Grants No. PHY 1913554, No. PHY 2209429, No. PHY 1430152, and No. PHY 1613188. This material is based upon work supported by the Department of Energy/National Nuclear Security Administration through the Nuclear Science and Security Consortium under Award No. DE-NA0003180, and Stewardship Science Academic Alliance under DE-NA0003906. A. C. L. gratefully acknowledges funding from the Research Council of Norway, Grant Project No. 316116. This work is based on the research supported in part by the National Research Foundation of South Africa (Grant No. 118846). This material is based upon work supported by the U.S. Department of Energy, Office of Science, Office of Nuclear Physics, under Contracts No. DE-AC02-06CH11357 and No. DE-SC0020451. This work was performed under the auspices of the U.S. Department of Energy by Lawrence Livermore National Laboratory under Contract No. DE-AC52-07NA27344. S. L. was supported by the Laboratory Directed Research and Development Program at Pacific Northwest National Laboratory operated by Battelle for the U.S. Department of Energy. This work is partly supported by the Research Council of Norway (Grant No. 263030). S. N. acknowledges funding from the European Union's Horizon 2020 research and innovation programme under Grant Agreement No. 771036 (ERC CoG MAIDEN). This research was partially supported by the Natural Sciences and Engineering Research Council (NSERC) of Canada. D. M. was supported by the FRIB Visiting Scholar Fellowship and the Norwegian Nuclear Research Centre (Grant Project No. 341985).

*spyrou@frib.msu.edu
†muecher@ikp.uni-koeln.de
‡NuGrid Collaboration; http://nugridstars.org

[1] E. M. Burbidge, G. R. Burbidge, W. A. Fowler, and F. Hoyle, Rev. Mod. Phys. **29**, 547 (1957).
[2] A. G. W. Cameron, Publ. Astron. Soc. Pac. **69**, 201 (1957).
[3] F. Käppeler, R. Gallino, S. Bisterzo, and W. Aoki, Rev. Mod. Phys. **83**, 157 (2011).
[4] M. Arnould, S. Goriely, and K. Takahashi, Phys. Rep. **450**, 97 (2007).
[5] C. Sneden, J. J. Cowan, and R. Gallino, Annu. Rev. Astron. Astrophys. **46**, 241 (2008).
[6] J. J. Cowan, C. Sneden, J. E. Lawler, A. Aprahamian, M. Wiescher, K. Langanke, G. Martínez-Pinedo, and F.-K. Thielemann, Rev. Mod. Phys. **93**, 015002 (2021).
[7] M. Arnould and S. Goriely, Phys. Rep. **384**, 1 (2003).
[8] J. J. Cowan and W. K. Rose, Astrophys. J. **212**, 149 (1977).
[9] M. Asplund, D. L. Lambert, T. Kipper, D. Pollacco, and M. D. Shetrone, Astron. Astrophys. **343**, 507 (1999), https://ui.adsabs.harvard.edu/abs/1999A%26A...343..507A/abstract.

[10] F. Herwig, M. Pignatari, P. R. Woodward, D. H. Porter, G. Rockefeller, C. L. Fryer, M. Bennett, and R. Hirschi, Astrophys. J. **727**, 89 (2011).

[11] S. Bisterzo, R. Gallino, O. Straniero, S. Cristallo, and F. Käppeler, Mon. Not. R. Astron. Soc. **422**, 849 (2012).

[12] L. Dardelet, C. Ritter, P. Prado, E. Heringer, C. Higgs, S. Sandalski, S. Jones, P. Denisenkov, K. Venn, M. Bertolli, M. Pignatari, P. Woodward, and F. Herwig, in *Proceedings of XIII Nuclei in the Cosmos (NIC XIII). 2014. Debrecen, Hungary* (PoS, 2014), p. 145, http://pos.sissa.it/cgi-bin/reader/conf.cgi?confid=204.

[13] S. Jones, C. Ritter, F. Herwig, C. Fryer, M. Pignatari, M. G. Bertolli, and B. Paxton, Mon. Not. R. Astron. Soc. **455**, 3848 (2015).

[14] M. Hampel, R. J. Stancliffe, M. Lugaro, and B. S. Meyer, Astrophys. J. **831**, 171 (2016).

[15] I. U. Roederer, A. I. Karakas, M. Pignatari, and F. Herwig, Astrophys. J. **821**, 37 (2016).

[16] M. Hampel, A. I. Karakas, R. J. Stancliffe, B. S. Meyer, and M. Lugaro, Astrophys. J. **887**, 11 (2019).

[17] R. A. Malaney, Mon. Not. R. Astron. Soc. **223**, 683 (1986).

[18] A. Jorissen and M. Arnould, Astron. Astrophys. **221**, 161 (1989), https://adsabs.harvard.edu/full/1989A%26A...221..161J.

[19] S. Cristallo, L. Piersanti, O. Straniero, R. Gallino, I. Dominguez, and F. Kappeler, Pub. Astron. Soc. Aust. **26**, 139 (2009).

[20] S. Cristallo, D. Karinkuzhi, A. Goswami, L. Piersanti, and D. Gobrecht, Astrophys. J. **833**, 181 (2016).

[21] D. Karinkuzhi, S. Van Eck, S. Goriely, L. Siess, A. Jorissen, T. Merle, A. Escorza, and T. Masseron, Astron. Astrophys. **645**, A61 (2021).

[22] P. Denissenkov, F. Herwig, U. Battino, C. Ritter, M. Pignatari, S. Jones, and B. Paxton, Astrophys. J. Lett. **834**, L10 (2017).

[23] P. Denissenkov, F. Herwig, P. Woodward, R. Andrassy, M. Pignatari, and S. Jones, Mon. Not. R. Astron. Soc. **488**, 4258 (2019).

[24] A. Choplin, L. Siess, and S. Goriely, Astron. Astrophys. **648**, A119 (2021).

[25] S. W. Campbell, M. Lugaro, and A. I. Karakas, Astron. Astrophys. **522**, L6 (2010).

[26] P. Banerjee, Y.-Z. Qian, and A. Heger, Astrophys. J. **865**, 120 (2018).

[27] P. A. Denissenkov, F. Herwig, G. Perdikakis, and H. Schatz, Mon. Not. R. Astron. Soc. **503**, 3913 (2021).

[28] A. Choplin, S. Goriely, and L. Siess, Astron. Astrophys. **667**, L13 (2022).

[29] J. E. McKay, P. A. Denissenkov, F. Herwig, G. Perdikakis, and H. Schatz, Mon. Not. R. Astron. Soc. **491**, 5179 (2020).

[30] S. Goriely, L. Siess, and A. Choplin, Astron. Astrophys. **654**, A129 (2021).

[31] A. Simon, M. Beard, A. Spyrou, S. J. Quinn, B. Bucher, M. Couder, P. A. DeYoung, A. C. Dombos, J. Görres, A. Kontos, A. Long, M. T. Moran, N. Paul, J. Pereira, D. Robertson, K. Smith, E. Stech, R. Talwar, W. P. Tan, and M. Wiescher, Phys. Rev. C **92**, 025806 (2015).

[32] S. Martinet, A. Choplin, S. Goriely, and L. Siess, Astron. Astrophys. **684**, A8 (2024).

[33] A. Spyrou, S. N. Liddick, A. C. Larsen, M. Guttormsen, K. Cooper, A. C. Dombos, D. J. Morrissey, F. Naqvi, G. Perdikakis, S. J. Quinn, T. Renstrøm, J. A. Rodriguez, A. Simon, C. S. Sumithrarachchi, and R. G. T. Zegers, Phys. Rev. Lett. **113**, 232502 (2014).

[34] S. N. Liddick *et al.*, Phys. Rev. Lett. **116**, 242502 (2016).

[35] M. Wiedeking, M. Guttormsen, A. C. Larsen, F. Zeiser, A. Görgen, S. N. Liddick, D. Mücher, S. Siem, and A. Spyrou, Phys. Rev. C **104**, 014311 (2021).

[36] D. Mücher *et al.*, Phys. Rev. C **107**, L011602 (2023).

[37] W. Hauser and H. Feshbach, Phys. Rev. **87**, 366 (1952).

[38] A. J. Koning, S. Hilaire, and M. C. Duijvestijn, in *TALYS1.6: Proceedings of the International Conference on Nuclear Data for Science and Technology, 2007, Nice, France*, edited by O. Bersillon, F. Gunsing, E. Bauge, R. Jacqmin, and S. Leray, EDP Sciences, 2008 (2007), pp. 211–214.

[39] T. Rauscher, P. Mohr, I. Dillmann, and R. Plag, Astrophys. J. **738**, 143 (2011).

[40] T. Rauscher, Astrophys. J. Suppl. Ser. **201**, 26 (2012).

[41] I. Dillmann, T. Szücs, R. Plag, Z. Fülöp, F. Käppeler, A. Mengoni, and T. Rauscher, Nucl. Data Sheets **120**, 171 (2014).

[42] A. Simon, S. Quinn, A. Spyrou *et al.*, Nucl. Instrum. Methods Phys. Res., Sect. A **703**, 16 (2013).

[43] M. Guttormsen, T. Ramsøy, and J. Rekstad, Nucl. Instrum. Methods Phys. Res., Sect. A **255**, 518 (1987).

[44] A. C. Larsen, M. Guttormsen, M. Krtička, E. Běták, A. Bürger, A. Görgen, H. T. Nyhus, J. Rekstad, A. Schiller, S. Siem, H. K. Toft, G. M. Tveten, A. V. Voinov, and K. Wikan, Phys. Rev. C **83**, 034315 (2011).

[45] A. Schiller, L. Bergholt, M. Guttormsen, E. Melby, J. Rekstad, and S. Siem, Nucl. Instrum. Methods Phys. Res., Sect. A **447**, 498 (2000).

[46] B. L. Berman, S. C. Fultz, J. T. Caldwell, M. A. Kelly, and S. S. Dietrich, Phys. Rev. C **2**, 2318 (1970).

[47] V. V. Varlamov, B. S. Ishkhanov, V. N. Orlin, and N. N. Peskov, Phys. At. Nucl. **79**, 501 (2016).

[48] H. Utsunomiya, T. Renstrøm, G. M. Tveten, S. Goriely, T. Ari-izumi, V. W. Ingeberg, B. V. Kheswa, Y.-W. Lui, S. Miyamoto, S. Hilaire, S. Péru, and A. J. Koning, Phys. Rev. C **100**, 034605 (2019).

[49] S. Goriely, S. Hilaire, S. Péru, and K. Sieja, Phys. Rev. C **98**, 014327 (2018).

[50] S. Goriely, P. Dimitriou, M. Wiedeking, T. Belgya, R. Firestone, J. Kopecky, M. Krtička, V. Plujko, R. Schwengner, S. Siem, H. Utsunomiya, S. Hilaire, S. Péru, Y. S. Cho, D. M. Filipescu, N. Iwamoto, T. Kawano, V. Varlamov, and R. Xu, Eur. Phys. J. A **55**, 172 (2019).

[51] A. C. Larsen and S. Goriely, Phys. Rev. C **82**, 014318 (2010).

[52] M. Guttormsen *et al.*, Phys. Rev. C **106**, 034314 (2022).

[53] R. Capote *et al.*, Nucl. Data Sheets **110**, 3107 (2009), special Issue on Nuclear Reaction Data.

[54] S. N. Liddick, A.-C. Larsen, M. Guttormsen, A. Spyrou *et al.*, Phys. Rev. C **100**, 024624 (2019).

[55] S. Goriely, S. Hilaire, and A. J. Koning, Phys. Rev. C **78**, 064307 (2008).
[56] R. H. Cyburt, A. M. Amthor, R. Ferguson, Z. Meisel, K. Smith, S. Warren, A. Heger, R. D. Hoffman, T. Rauscher, A. Sakharuk, H. Schatz, F. K. Thielemann, and M. Wiescher, Astrophys. J. Suppl. Ser. **189**, 240 (2010).
[57] D. Stephens, F. Herwig, P. Woodward, P. Denissenkov, R. Andrassy, and H. Mao, Mon. Not. R. Astron. Soc. **504**, 744 (2021).
[58] A. Abohalima and A. Frebel, Astrophys. J. Suppl. Ser. **238**, 36 (2018).
[59] T. C. Beers and N. Christlieb, Annu. Rev. Astron. Astrophys. **43**, 531 (2005).